Suan Sunandha Science and Technology Journal

Study of the Effect of Doping Dysprosium Ions in Soda Lime Silicoborate Glasses Using Microwave Technique for White Light-emitting Diodes (WLEDs)

Nattaporn Mahingsa, Watcharin Rachniyom, Keerati Kirdsiri, Nattapon Srisittiposakun*

Physics Program, Faculty of Science and Technology, Nakhon Pathom Rajabhat University, Nakhon Pathom 7300, Thailand

***Corresponding author e-mail: Nattapon2004@gmail.com**

Received: *2 January 2025* / **Revised:** *17 March 2025* / **Accepted:** *18 April 2025*

Abstract

Soda lime silicoborate glasses doped with dysprosium ions (Dy^{3+}) were synthesized with a glass composition of $55.0B_2O_3$: $25.0SiO_2$: $10.0Na_2O$: 10.0CaO: xDy_2O_3 (where x represents the concentration of Dy_2O_3, varying from 0.0 to 2.0 mol%). The synthesis was carried out using a microwave technique and the physical, optical and luminescence properties of the obtained glasses were investigated. The results showed that the density and refractive index increased, while the molar volume decreased with higher Dy_2O_3 concentration. The absorption spectra indicated that these glasses exhibited absorption in the UV-visible and near-infrared light regions. When excited at 388 nm, the glass emitted light at wavelengths of 481, 575, and 663 nm. The emission intensity increased with increasing Dy_2O_3 concentration up to 0.5 mol%, after which it decreased due to the concentration quenching effect. The CIE 1931 chromaticity diagram confirmed that the glasses emitted light in the white region. Likewise, the glasses exhibited CCT values that fall within the bright white color region, with temperature values ranging from 4309 to 4393 K. The Y/B ratio was calculaed from the luminscence spectraindicating the level of asymmetry in the prepared glasses. The decay time showed a non-exponential behavior, indicating cross -relaxation between Dy^{3+}-Dy^{3+} ions, and the decay curve was fitted using the IH model S = 10 (quadrupole-quadrupole). The Judd-Ofelt (JO) parameters (Ω_2, Ω_4 and Ω_6) were calculated from the absorption spectra, and the radiative transition probabilities (A_R), stimulated emission cross-sections ($\sigma(\lambda_p)$) and branching ratios (β_R) were obtained from the JO parameters. The results confirm the suitability of these glass samples for use in WLEDs and as laser medium.

Keywords: Dysprosium ions, Soda lime borosilicate, Glass, Luminescence, White-light application, Microwave technique

1. Introduction

In recent decades, photonic devices such as light bulbs, displays screens, optical sensors, scintillation detectors, optical fibers, and lasers have become integral parts of our daily lives (Kashif & Ratep, 2022). Presently, the quantum computing revolution, which harnesses photons instead of electrons, promises to revolutionize technology once more, significantly expanding the applications of photonics (Kaewnuam et al., 2017; Sreedhar et al., 2013; Venkata Rao et al., 2015). White light emitting diodes (W-LEDs) have found extensive application in diverse scientific and technological domains, such as telecommunications, medical science, barcode reading, and biolabeling (Srihari & Jayasankar, 2017). W-LEDs have garnered considerable interest in the field of solid-state lasers (SSLs) owing to their superior performance characteristics, including high luminous efficiency, low power dissipation, long operational lifetime, reliability, and excellent low-temperature efficiency (Ichoja et al., 2020; Krishnaiah et al., 2013; Rajagukguk et al., 2020).

Dysprosium ions (Dy^{3+}), a rare earth ion, is an excellent option for white light applications due to its two prominent emission bands $^4F_{9/2} \rightarrow {}^6H_{15/2}$ and $^4F_{9/2} \rightarrow {}^6H_{13/2}$. These energy level transitions emit light within the visible spectrum, making dysprosium particularly suitable for producing white light (Monisha et al., 2021). The

$^4F_{9/2} \rightarrow {}^6H_{15/2}$ emission band in dysprosium arises from a magnetic dipole transition, while the $^4F_{9/2} \rightarrow {}^6H_{15/2}$ emission band is due to an electric dipole transition. The intensity of the yellow emission band ($^4F_{9/2} \rightarrow {}^6H_{13/2}$) is significantly influenced by the ligand field surrounding the Dy^{3+} ion (Kashif & Ratep, 2022). By carefully adjusting the glass composition, Dy^{3+} ion concentration, and excitation wavelengths, it is possible to manipulate the yellow-to-blue (Y/B) intensity ratio and achieve white light emission from Dy^{3+}-doped glass materials (Rajagukguk et al., 2020).

Glass melting is commonly performed using electric furnaces, which offer advantages in terms of precise temperature control and a cleaner melting process. however, melting glass with electric furnaces comes with high costs, requiring a significant amount of electricity, environmental impacts from electricity sources, and high maintenance expenses (Sevast'yanov, 1994). Therefore, researchers are interested in reducing costs by using microwave furnaces as an alternative (Mandal et al., 2013). Also, microwave ovens are compact, refractory-lined appliances specifically designed to fit within standard household microwave ovens. Microwave ovens use microwave radiation to heat glass during the melting process, requiring less time (Mahmoud et al., 2012). They are also convenient, safe, and energy-efficient for creating small glass pieces and producing glass for optical applications. Glass melting using microwave technology saves time, reduces production costs, and is more energy-efficient compared to electric furnaces (Kumar et al., 2017).

In this work, dysprosium ions doped soda lime silicoborate glass were fabricated using microwave melting technique. The physical, optical and luminescence properties were investigated. Therefore, studying the luminescence properties of Dy^{3+} ions in glass is of interest for their potential application in white light-emitting diodes (WLEDs) and laser medium.

2. Materials and Methods

The dysprosium ions doped soda lime silicoborate glass (called the BSDy glasses) was prepared in this present work using the microwave technique with the composition shown in Table 1. A total of 15g of chemical powders were mixed in an alumina crucible, placed in a microwave kiln and heated at 1,000 W for 35 minutes in a microwave oven. afterward the molten mixture was cast into a rectangular graphite mold and then brought to anneal at 500°C for 3 hours in an electric furnace. The process was repeated until all the samples were obtained. The samples were then cut and polished using jewelry polishing materials into approximately 1.0 x 1.5 x 0.3 cm^3 for further investigations.

Table 1. The nominal composition of glass samples.

Samples	Glass compositions (mol%)
0.0BSDy	$55.0B_2O_3$: $25.0SiO_2$: $10.0Na_2O$: 10.0CaO: $0.0Dy_2O_3$
0.3BSDy	$54.7B_2O_3$: $25.0SiO_2$: $10.0Na_2O$: 10.0CaO: $0.3Dy_2O_3$
0.5BSDy	$54.5B_2O_3$: $25.0SiO_2$: $10.0Na_2O$: 10.0CaO: $0.5Dy_2O_3$
1.0BSDy	$54.0B_2O_3$: $25.0SiO_2$: $10.0Na_2O$: 10.0CaO: $1.0Dy_2O_3$
1.5BSDy	$53.5B_2O_3$: $25.0SiO_2$: $10.0Na_2O$: 10.0CaO: $1.5Dy_2O_3$
2.0BSDy	$53.0B_2O_3$: $25.0SiO_2$: $10.0Na_2O$: 10.0CaO: $2.0Dy_2O_3$

The important parameters such as density were investigated using the Archimedes method (Meejitpaisan et al., 2021) and distill water as the reference liquid. The refractive index was measured using Abbe refractometer with sodium vapor as the light source with a filter wavelength of 589.3 nm. The Absorption spectra were measured in the wavelength range of 300-1900 nm using Shimadzu UV-3600, UV-VIS-NIR instrument. The photoluminescence spectra and decay time were recorded by Cary eclipse spectrometer. All measurements were conducted at room temperature.

3. Results and Discussion

3.1 Physical properties

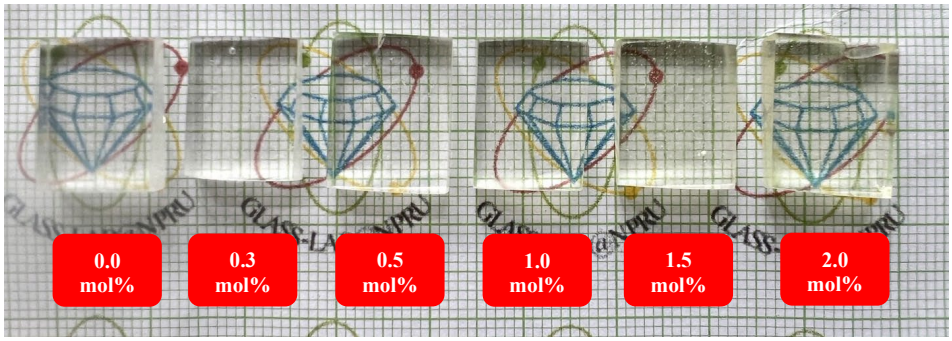

Figure 1. The picture of BSDy glasses doped with dysprosium ions.

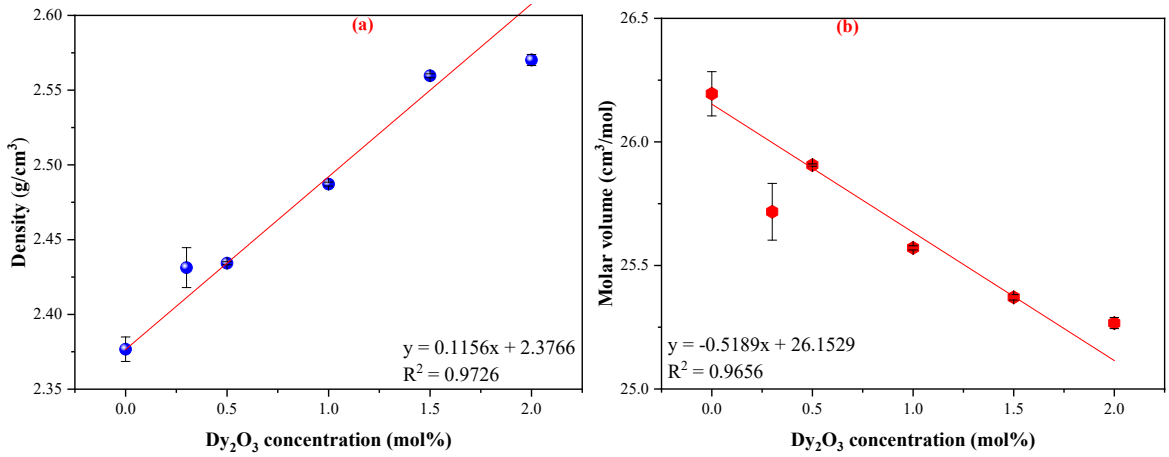

Figure 2. The (a) density and (b) molar volume of BSDy glasses doped with dysprosium ions.

The appearance of the BSDy glass samples was displayed in Figure 1, It was found that the glasses have slightly yellow color with an increase in Dy_2O_3 concentration. It also shows the high transparency. For the density investigation, it increased with increasing dysprosium dioxide concentration due to dysprosium dioxide is heavier than boron dioxide (Kaewnuam et al., 2017). Hence, the substitution of boron dioxide by dysprosium dioxide in higher concentration influences the increase in density of glasses, The addition of Dy_2O_3 into the glass structure results in an expansion of the molar volume. The Dy^{3+} ions act as network modifiers, the glass creates non-bridging oxygen (NBO) when incorporated into glass network as shown in Figure 2 (b) (Insitipong et al., 2011).

3.2 Optical properties

As the density increases, correspondingly the speed of light decreases (due to n=c/v), leading to an increase in the refractive index from 1.584 to 1.657 with increasing Eu^{3+} concentration (Singkiburin et al., 2023; Zaman et al., 2019) found that when the concentration of dysprosium increased, the refractive index also increased.

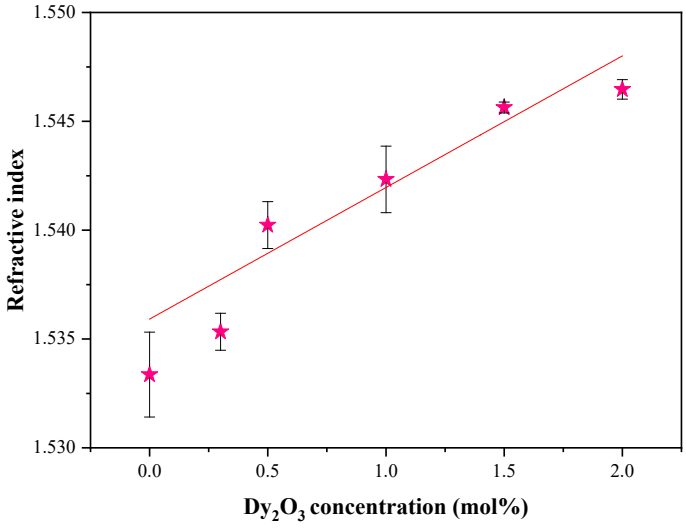

Figure 3. The refractive index of BSDy glasses doped with dysprosium ions.

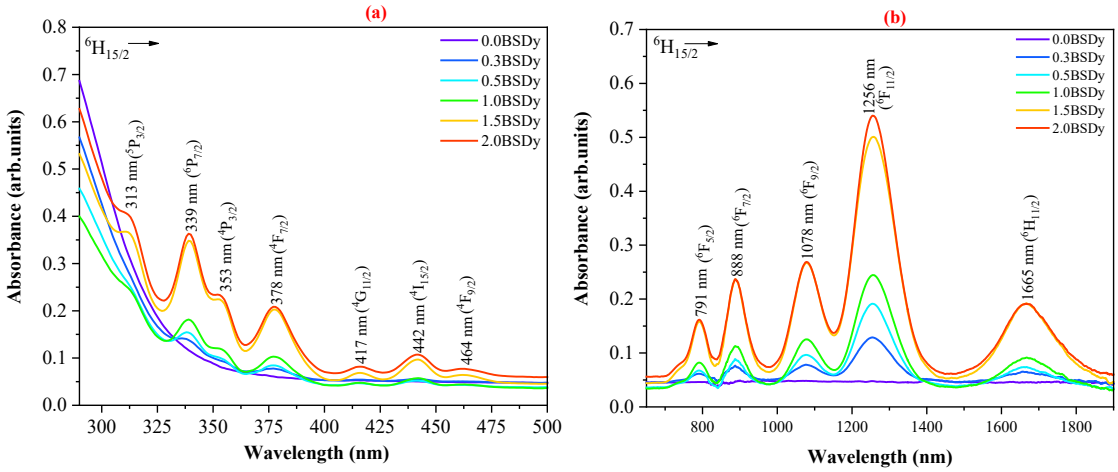

Figure 4. The absorption spectra in (a) UV-VIS and (b) NIR regions of BSDy glasses doped with dysprosium ions.

Figure 4 displayed the absorption spectra in (a) UV-VIS to (b) NIR regions, observed in Dy^{3+} doped BSDy glasses. The several characteristic bands, such as 313, 339, 353, 378, 417, 442, 465, 791, 888, 1078, 1256 and 1665 nm are interrelated to $^6H_{15/2} \rightarrow {}^5P_{3/2}$, $^6P_{7/2}$, $^4P_{3/2}$, $^4F_{7/2}$, $^4G_{11/2}$, $^4I1_{5/2}$, $^4F_{9/2}$, $^6F_{5/2}$, $^6F_{7/2}$, $^4F_{9/2}$, $^4F_{11/2}$ and $^6H_{11/2}$ transitions, respectively (Zaman et al., 2019).

3.3 Luminescence properties

The emission spectra were examined with an excitation wavelength of 350 nm (as depicted in Figure 5). three peaks were observed at 481 ($^6H_{15/2}$), 575 ($^6H_{13/2}$) and 663 nm ($^6H_{11/2}$) (Monisha et al., 2021), with the strongest emission occurring at 575 nm wavelength. From energy level diagram, transitions between the $^6P_{7/2}$ and $^4F_{9/2}$ energy levels of Dy^{3+} ions typically involve non-radiative relaxation, as the small energy gap facilitates efficient energy transfer to lattice vibrations (Kıbrıslı et al., 2019; Venugopal et al., 2021). In contrast, transitions from the $^4F_{9/2}$ level to lower-lying levels, such as $^6H_{15/2}$, $^6H_{13/2}$, and $^6H_{11/2}$, result in radiative decay, emitting photons at wavelengths of 481 nm (yellow), 575 nm (blue), and 663 nm (red), respectively, and exhibited various non-radiative relaxation processes, including resonant energy transfer and cross-relaxation, which can compete with radiative decay and influence the overall luminescence efficiency of Dy^{3+} ions (Fernández-Rodríguez et al., 2023; Sun et al., 2020). This process, known as cross-relaxation energy transfer, involves multiple Dy^{3+} ions and

eventually leads to all involved ions returning to their ground state, resulting in luminescence. The cross-relaxation channels (CRCs) among Dy^{3+}, denoted as CRC1, CRC2, and CRC3 in Figure 6, become more significant at concentrations above 0.5 mol%, as the increased number of Dy^{3+} ions facilitated more frequent resonant energy transfer between donor and acceptor ions. This enhanced energy transfer results in concentration quenching, leading to a decrease in the intensity of the emission peaks (Kıbrıslı et al., 2019). In addition, it was found that emission intensity increased when the concentration of Dy_2O_3 increased until it reached 0.5 mol% (Gökçe & Koçyiğit, 2019). After that, emissions were decreased, which is the phenomenon of concentration quenching effect. Therefore, the most appropriate concentration for doping Dy^{3+} into BSDy glass is 0.5 mol% (Monisha et al., 2021; Pugliese et al., 2016).

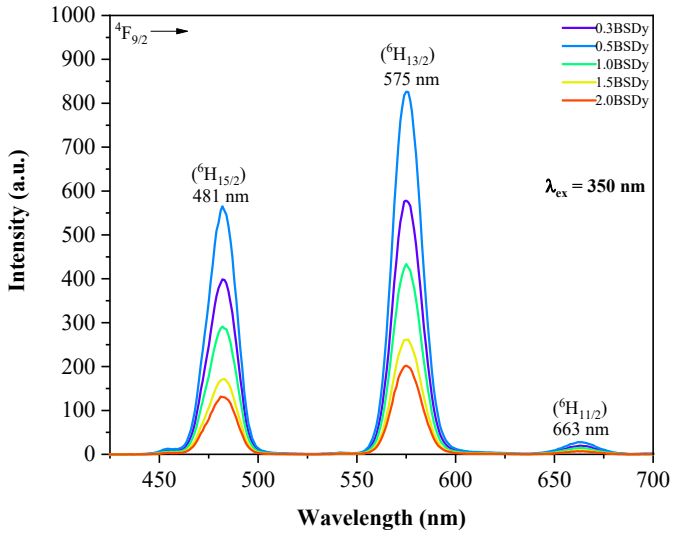

Figure 5. The emission spectra of BSDy glasses doped with dysprosium ions.

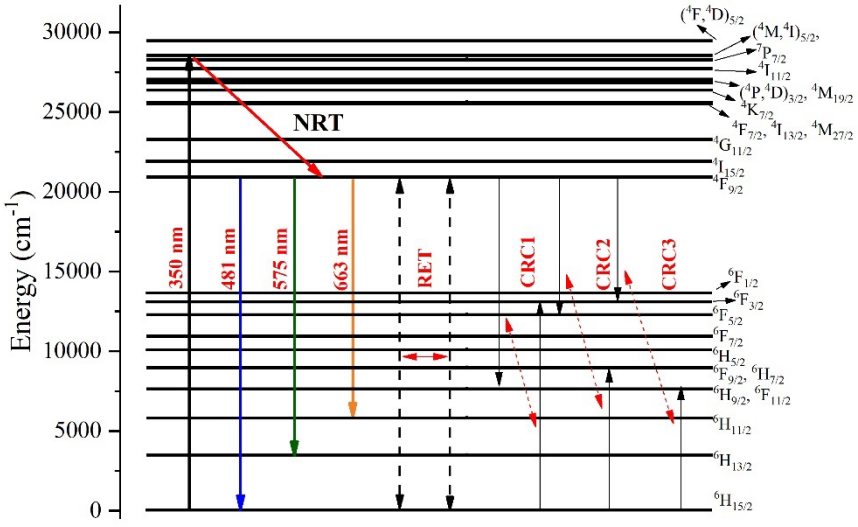

Figure 6. Energy levels diagram of BSDy glasses doped with dysprosium ions (Khan et al., 2019).

The excitation spectra of BSDy glasses were displayed in Figure 7. These spectra were investigated by keeping the emission wavelength at 575 nm, which is the highest peak in PL emission spectra. The excitation spectra exhibited 7 distinct sharp peaks, which correspond to the 4f-4f transitions of Dy^{3+} ions. These peaks originate from the ground state level, specifically from the $^6H_{15/2}$ level, and transition to various higher excited states (Pawar, Munishwar, & Gedam, 2017). The observed peaks in the excitation spectra are located at specific

wavelengths: 324 ($^6H_{15/2}\rightarrow{}^6P_{3/2}$), 350 ($^6H_{15/2}\rightarrow{}^6P_{7/2}$), 363 ($^6H_{15/2}\rightarrow{}^4P_{3/2}$), 387 ($^6H_{15/2}\rightarrow{}^4F_{7/2}$), 426 ($^6H_{15/2}\rightarrow{}^4G_{11/2}$), 451 ($^6H_{15/2}\rightarrow{}^4I1_{5/2}$), and 471 nm ($^6H_{15/2}\rightarrow{}^4F_{9/2}$), as illustrated in Figure 7.

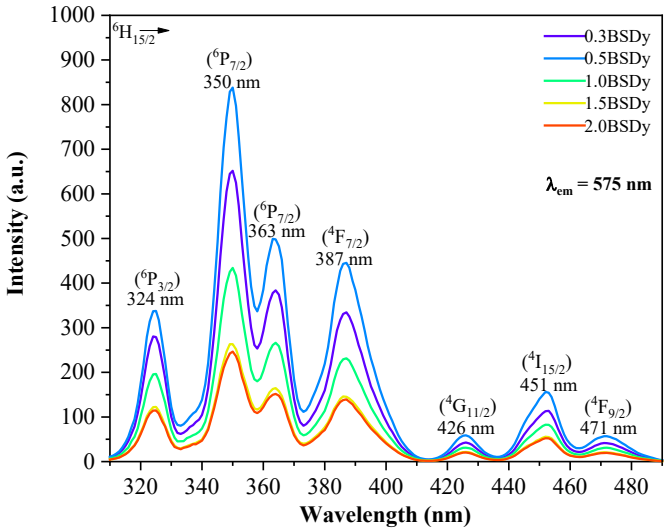

Figure 7. The excitation spectra of BSDy glasses doped with dysprosium ions.

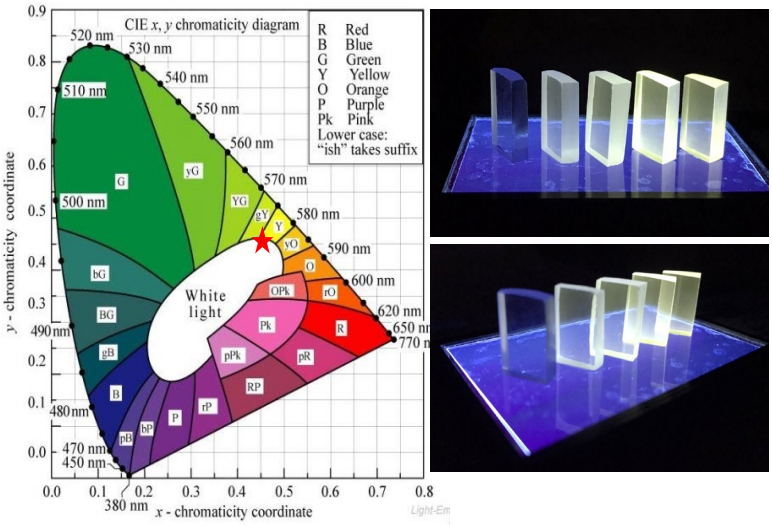

Figure 8. The CIE-1931 chromaticity diagram presents the color coordinates for Dy_2O_3 doped glasses.

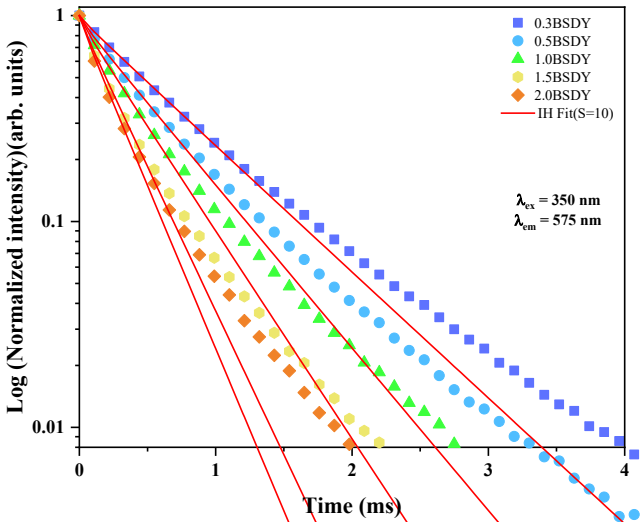

Figure 9. Decay time of BSDy glasses under excitation 350 and emission 575 nm.

The CIE 1931 chromaticity coordinates (x, y), an internationally recognized system for specifying color, can be used to analyze the color of light and these values are shown in Figure 8 (Poonam et al., 2020). The analysis of color coordinates indicated from the PL emission spectra under 350 nm excitation was used to calculate the color of emitted light. The yellow-to-blue (Y/B) intensity ratio has been used to determine the degree of covalency of the Dy^{3+}- O^{2-} bond. In this study, the Y/B ratios were calculated for all the prepared glasses. The results, along with other reports (Pawar, Munishwar, Gautam, & Gedam, 2017; Rao et al., 2000), displayed that the addition of Dy^{3+} ions to the glass matrix strongly influences the local environment, leading to hypersensitive yellow emission (Hong et al., 2024) as shown in Table 2. Y/B ratio indicated trends of increased when adding Dy^{3+} concentration. Furthermore, CCT can be evaluated by equation represent by McCamy as follows (Alhodaib et al., 2021):

$$CCT = -449n^3 + 352n^2 - 682n + 5520.33 \quad [1]$$

With the constant defined as (x_e=0.332, y_e=0.186) and n calculated as ($x-x_e$) divided by ($y-y_e$), The correlated color temperature (CCT) is a crucial parameter that describes the color characteristics of light emitted from luminescent materials, and it is measured in Kelvin (K). The calculated CCT values for the prepared glass were obtained by referencing relevant literature (Monisha et al., 2021; Venugopal et al., 2021). Based on these values, white light can be categorized into three ranges: (i) warm white light (2700–4000 K), (ii) bright white light (4000–5000 K), and (iii) cool white light (5000 K and above)(Srihari and Jayasankar 2017). For this study, the obtained CCT values were in the range of 4000–4500 K, indicating that the glass is close to the bright white light range shown in Table 2. Hence, all these samples used as white light source. The non-exponential decay in Dy^{3+} doped glasses with concentrations ranging from 0.3 to 1.5 mol% indicated energy transfer via cross-relaxation between Dy^{3+} ions, resulting in a decreased in decay time with increasing Dy^{3+} concentration (Kaewnuam et al., 2017). The increased interaction between Dy^{3+} ions lead to energy transfer among Dy^{3+} ions, resulting in a deviation from single exponential decay. In this step, the non-exponential decay behavior was analyzed using the Inokuti-Hirayama (IH) model to understand the underlying interaction mechanism as discussed in (Shoaib et al., 2020; Vijayakumar et al., 2015). The Inokuti-Hirayama (IH) model, employed to analyze energy transfer between Dy^{3+} ions (Ichoja et al., 2020), is applicable when energy transfer between donor and acceptor ions significantly outpaces energy diffusion among donors. Based on IH theory, the emission intensity can be described as (Vijayakumar & Marimuthu, 2015)

$$I(t) = I_0 \exp\left\{\frac{-t}{\tau_0} - Q\left(\frac{t}{\tau_0}\right)^{3/s}\right\} \quad [2]$$

where S represents the interaction type (6 for dipole-dipole, 8 for dipole-quadrupole, and 10 for quadrupole-quadrupole) between Dy^{3+} ions, t denotes the time elapsed since excitation, τ_0 signifies the intrinsic decay time of donors in the absence of acceptors, and Q is the defined energy transfer parameter.

$$Q = \frac{4\pi}{3}\gamma\left(1 - \frac{3}{s}\right)N_0 R_0^3 \quad [3]$$

Therefore, the IH model fitting for S=10, as shown in Figure 9, shown excellent concordantly with experimental data, indicating the presence of quadrupole-quadrupole interactions between Dy^{3+} ions (Shoaib et al., 2020). The decay time was observed to decrease with increasing Dy^{3+} concentration, while the energy transfer parameter (Q) increased. So, the increase in these Q values corresponds to the higher concentration of Dy^{3+} ions, as mentioned. The cross-relaxation and resonance energy transfer processes between Dy^{3+}-Dy^{3+} ions result in a reduction of the radiative decay time of Dy^{3+} ions in these glasses (Sarumaha et al., 2025; Vijayakumar et al., 2014).

Table 2. The CIE 1931 chromaticity, Correlated Color Temperature (CCT) and luminesce decay times.

Samples	CIE 1931		CCT (K)	Y/B ratio	τ (ms)	Q	R^2
	x	y					
0.3BSDy	0.3719	0.4065	4393	1.4632	0.7140	0.0486	0.9988
0.5BSDy	0.3733	0.4083	4364	1.5042	0.5550	0.0778	0.9977
1.0BSDy	0.3732	0.4084	4369	1.4964	0.4350	0.0853	0.9964
1.5BSDy	0.3757	0.4111	4318	1.5563	0.3140	0.0840	0.9951
2.0BSDy	0.3763	0.4120	4309	1.5697	0.2780	0.0868	0.9942

3.4 Judd-Ofelt parameters and oscillator strength

The oscillator strength is a crucial parameter that indicates the intensity of absorption in a system. It is measured by the area under the absorption peak in a spectrum. This area provides valuable information about electronic transitions and radiative properties, as described by the following relationship (Ratep & Kashif, 2023):

$$f_{exp} = 4.318 \times 10^{-9} \int \propto (v)dv \quad [4]$$

The Judd-Ofelt theory is a theoretical approach used to calculate electric dipole transitions in rare-earth ion systems within solid-state materials, particularly crystals or glasses. This theory enables us to describe and calculate the probability of electronic transitions between the ground state ΨJ and the excited state Ψ′J′.

$$f_{cal} = \frac{8\pi^2 mc(n^2+1)^2}{3h\lambda(2J+1)9n}\sum_{\lambda=2,4,6}\Omega_\lambda(\psi J \parallel U^\lambda \parallel \varphi' J')^2 \quad [5]$$

The root mean square deviation (RMSD) can be calculated from the following relationship:

$$\delta_{rms} = \left[\frac{\sum(fexp - fcal)^2}{N-3}\right]^{\frac{1}{2}} \quad [6]$$

Table 3. Oscillator strengths, both experimental (f_{exp}) and calculated (f_{cal}), for 0.5BSDy glass are provided along the band position wavelengths (nm) and corresponding energy (cm^{-1}).

Transitions $^6H_{15/2}\rightarrow$	f_{exp} (x 10^{-6})	f_{cal} (x 10^{-6})
$^6P_{7/2}$	0.3716	0.5532
$^4P_{3/2}$	3.5050	3.4810
$^4F_{7/2}$	0.9697	1.0177
$^4G_{11/2}$	1.0330	0.8466
$^4I_{15/2}$	0.6727	0.3746
$^4F_{9/2}$	0.0740	0.0643
$^6F_{5/2}$	0.1657	0.1885
$^6F_{7/2}$	0.0485	0.0329
$^6F_{9/2}$	0.4320	0.3194
$^6F_{11/2}$	0.2525	0.1189
$^6H_{11/2}$	0.6396	0.0222
$\Omega_2 = 7.974 \times 10^{-20}$ $\Omega_4 = 0.966 \times 10^{-20}$ $\Omega_6 = 0.934 \times 10^{-20}$ RMS = 0.241		

The experimental oscillator strength (f_{exp}) of 0.5 mol% Dy^{3+} doped glass (0.5BSDy) was calculated by integrating the peak area of the absorption spectra and using the formula from previous research (Poonam et al., 2020; Rajagukguk et al., 2021). The J-O parameters (Ω_λ), where λ are 2, 4, and 6, were determined using the experimental oscillator strength (f_{exp}) through least square fitting with the J-O theory equation research (Poonam et al., 2020; Rajagukguk et al., 2021). These parameters were turn back directly into same equation to identify the calculated oscillator strength (f_{cal}), Table 3 presented the f_{exp} and f_{cal} values for 0.5BSDy glass from this study and some reports (Rajagukguk et al., 2021; Wantana et al., 2016). The higher Ω_2 parameter indicates that 0.5BSDy glass has a highly asymmetric environment and a higher covalency with surround atoms compared to other systems. From this Table 3, it is observed that the Ω_4 and Ω_6 values of 0.5BSDy glass are higher than those of other systems displayed in Table 4, which correlates to higher viscosity and rigidity of the glass (Abdullahi et al., 2023; Ahmadi et al., 2020; Amjad et al., 2013; Wantana et al., 2016).

Table 4. Comparison of Judd–Ofelt parameters ($\Omega_{\lambda=2,4,6} \times 10^{-20}$) of Dy^{3+} in different samples.

Samples	Ω_2	Ω_4	Ω_6	Trend
This work	7.974	0.966	0.934	$\Omega_2>\Omega_4>\Omega_6$
G4 (Amjad et al., 2013)	4.628	0.774	0.794	$\Omega_2>\Omega_4>\Omega_6$
STAMB1(Abdullahi et al., 2023)	1.290	0.347	0.241	$\Omega_2>\Omega_4>\Omega_6$
Zinc-phosphate (Ahmadi et al., 2020)	2.210	0.530	0.510	$\Omega_2>\Omega_4>\Omega_6$

Table 5. Emission peak wavelength (λp, nm), effective band width ($\Delta\lambda_{eff}$, nm), radiative transition probability (A_R (s^{-1})), stimulated emission cross-section (σ x 10^{-20}) cm^2), experimental and calculation branching ratios (β_R) for 0.5BSDy glass.

Transitions	λ_p (nm)	A_R (s^{-1})	σ (x 10^{-20}) cm^2	$\beta_{R(exp)}$	$\beta_{R(cal)}$
$^6H_{15/2}$	481	68.50	2548.9	0.38	0.81
$^6H_{13/2}$	575	307.90	3695.5	0.60	0.61
$^6H_{11/2}$	662	41.18	1222.2	0.02	0.14

Tabel 6. Peak wavelength (λ_p, nm), stimulated emission cross section [σ (λ_p) x 10^{-22}, cm^2], radiative transition probability (A_R, s^{-1}) and branching ratio (β_R) compared with other values reported in the literature

Samples	λ_p (nm)	A_R (s^{-1})	σ (x 10^{-22}) cm^2	β_R	
				Exp	cal
0.5BSDy (Present work)	575	396.50	68.50	0.60	0.61
LFB-Dy07 (Wantana et al., 2016)	575	1245.11	5.29	0.53	0.70
OFLZBSD1.0 (Poonam et al., 2020)	575	-	37.30	0.52	0.62
LANKPD (Rajagukguk et al., 2021)	572	266.54	1.198	0.58	0.62
LiLaB; Dy^{3+} (Wantana et al., 2016)	575	649.98	21.93	0.58	0.52

The data obtained from Ω_λ, refractive index, and emission spectra were used to calculate the radiative transition probability (A), stimulated emission cross section (σ), and branching ratio (β_R) of 0.5BSDy glass. All processes and relevant equations were applied using the J-O theory (Kaewnuam et al., 2017), and the results are presented in Table 5. The branching ratio plays a critical role in determining the potential for stimulated emission from any transition (Khan et al., 2019; Shoaib et al., 2020), the $^4F_{9/2} \rightarrow {}^6H_{13/2}$ transition consistently displays calculated and experimental branching ratios (β_R) more than 0.50 for 0.5BSDy, suggesting its strong potential for laser emission. Furthermore, the high values of stimulated emission cross-section ($\sigma(\lambda_P)$) and radiative transition probability (A_R) associated with this transition further reinforce its suitability for laser applications (Monisha et al., 2021; Venugopal et al., 2021). Furthermore, Table 6 provided a comprehensive comparison of the radiative properties of 0.5BSDy glass samples with those of other previously reported Dy^{3+}-doped glasses.

4. Conclusions

The current study extensively describes the physical, optical, and luminescent characteristics of Dy^{3+} ions doped in BSDy glasses with formular $55.0B_2O_3$: $25.0SiO_2$: $10.0Na_2O$: 10.0CaO: xDy_2O_3 (where x varying contents from 0.0 to 2.0 mol%). The density increased as the concentration of Dy_2O_3 increased, but the molar volume decreased with increasing concentration of Dy_2O_3. The decreased in molar volume with increasing Dy_2O_3 concentration indicated that Dy^{3+} ions bond with bridging oxygens, which reducing the gab in the glass network. From the absorption measurements, it was found 12 absorption peaks occurred. As the concentration of Dy_2O_3 increases, the absorption intensity of the BSDy glasses also increased. Characteristic Dy^{3+} peaks are observed in the photoluminescence excitation spectra. The intensities of these peaks increase with the Dy^{3+} ion concentration up to 0.5 mol% and then decreased, this decreased due to the quenching effect of the concentration. The CIE 1931 chromaticity coordinates of BSDy glasses correspond to the white light region. The measured CCT indicated cool nature, and the CCT values of the samples were above 4000 K. Y/B ratio in the studied glasses exhibited an increasing trend with the increasing concentration of Dy^{3+} ions, which can be attributed to the enhanced covalency of the Dy^{3+}-O^{2-} bond. To complement the experimental optical properties, the decay time results indicated an extended decay time measured in milliseconds. The non-exponential decay rates can be well-fitted to the Inokuti–Hirayama (IH) model for S=10, suggesting a quadrupole – quadrupole energy transfer mechanism between Dy^{3+} ions. The Judd-Ofelt theoretical evaluation was conducted for 0.5BSDy glass. A trend was observed in the Judd-Ofelt intensity parameters (Ω_2, Ω_4, Ω_6): $\Omega_2 > \Omega_4 > \Omega_6$. The higher Ω_2 parameter in this glass reflects the ligands surrounding Dy^{3+} ions in the 0.5BSDy glass, indicating asymmetry in its luminescence capability. Furthermore, the color purity achieved by BSDy glasses, which closely resembles daylight, suggests the high quality of the emitted light they emit, making them appropriate for white light-emitting diodes (WLEDs) and laser medium.

Acknowledgements

The authors gratefully acknowledge the support of Nakhon Pathom Rajabhat University, which provided essential facilities and a nurturing environment that significantly contributed to the completion of this work.

References

Abdullahi, I., Hashim, S., Sayyed, M. I., & Ghoshal, S. K. (2023). Intense up-conversion luminescence from Dy^{3+}-doped multi-component telluroborate glass matrix: Role of CuO nanoparticles embedment. *Heliyon, 9*(5), e15906. https://doi.org/10.1016/j.heliyon.2023.e15906

Ahmadi, F., Asgari, A., & Ghoshal, S. K. (2020). Calcium oxide modifier stimulated intense luminescence from Dy^{3+} doped in sulfophosphate glasses. *Optik, 224*, 165665. https://doi.org/ 10.1016/j.ijleo.2020.165665

Alhodaib, A., Ibrahim, O., Abd El All, S., & Ezzeldin, F. (2021). Effect of rare-earth ions on the optical and PL properties of novel borosilicate glass developed from agricultural waste. *Materials, 14*(19), 5607. https://doi.org/10.3390/ma14195607

Amjad, R. J., Sahar, M. R., Ghoshal, S. K., Dousti, M. R., & Arifin, R. (2013). Synthesis and characterization of Dy^{3+} doped zinc–lead-phosphate glass. *Optical Materials, 35*(5), 1103–1108. https://doi.org/10.1016/j.optmat.2012.12.024

Fernández-Rodríguez, L., Balda, R., Fernández, J., Durán, A., & Pascual, M. J. (2023). Structure and luminescent properties of Sm/Dy-doped $Sr_2MgSi_2O_7$ glass–ceramics. *International Journal of Applied Glass Science, 14*(1), 140–154. https://doi.org/10.1111/ijag.16584

Gökçe, M., & Koçyiğit, D. (2019). Spectroscopic investigations of Dy^{3+} doped borogermanate glasses for laser and wLED applications. *Optical Materials, 89*, 568–575. https://doi.org/10.1016/j.optmat.2019.02.004

Hong, Z., Yue, H., Luo, X., Gong, G., Lai, F., Zou, Z., You, W., Wu, S., & Huang, J. (2024). Spectroscopic studies of Dy^{3+} ions doped gallium silicate glasses for yellow solid-state lasers. *Silicon, 16*(1), 463–470. https://doi.org/10.1007/s12633-023-02693-z

Ichoja, A., Hashim, S., Ghoshal, S. K., & Hashim, I. H. (2020). Absorption and luminescence spectral analysis of Dy^{3+}-doped magnesium borate glass. *Chinese Journal of Physics, 66*, 307–317. https://doi.org/10.1016/j.cjph.2020.03.029

Insitipong, S., Kaewkhao, J., Ratana, T., & Limsuwan, P. (2011). Optical and structural investigation of bismuth borate glasses doped with Dy^{3+}. *Procedia Engineering, 8*, 195–199. https://doi.org/10.1016/j.proeng.2011.03.036

Kaewnuam, E., Wantana, N., Kim, H. J., & Kaewkhao, J. (2017). Development of lithium yttrium borate glass doped with Dy^{3+} for laser medium, W-LEDs and scintillation materials applications. *Journal of Non-Crystalline Solids, 464*, 96–103. https://doi.org/10.1016/j.jnoncrysol.2017.03.027

Kashif, I., & Ratep, A. (2022). Judd-Ofelt and luminescence study of dysprosium-doped lithium borosilicate glasses for lasers and w-LEDs. *Boletin de La Sociedad Espanola de Ceramica y Vidrio, 61*(6), 622–633. https://doi.org/10.1016/j.bsecv.2021.06.001

Khan, I., Rooh, G., Rajaramakrishna, R., Srisittipokakun, N., Kim, H. J., Kaewkhao, J., & Ruangtaweep, Y. (2019). Photoluminescence properties of Dy^{3+} ion-doped Li_2O-PbO-Gd_2O_3-SiO_2 glasses for white light application. *Brazilian Journal of Physics, 49*(5), 605–614. https://doi.org/10.1007/s13538-019-00695-0

Kıbrıslı, O., Ersundu, A. E., & Çelikbilek Ersundu, M. (2019). Dy^{3+} doped tellurite glasses for solid-state lighting: An investigation through physical, thermal, structural and optical spectroscopy studies. *Journal of Non-Crystalline Solids, 513*, 125–136. https://doi.org/10.1016/j.jnoncrysol.2019.03.020

Krishnaiah, K. V., Kumar, K. U., & Jayasankar, C. K. (2013). Spectroscopic properties of Dy^{3+}-doped oxyfluoride glasses for white light emitting diodes. *Materials Express, 3*(1), 61–70. https://doi.org/10.1166/mex.2013.1094

Kumar, D., Rao, S. M., & Singh, S. P. (2017). Structural, optical and thermoluminescence study of Dy^{3+} ion doped sodium strontium borate glass. *Journal of Non-Crystalline Solids, 464*, 51–55. https://doi.org/10.1016/j.jnoncrysol.2017.03.029

Mahmoud, M. M., Folz, D. C., Suchicital, C. T. A., & Clark, D. E. (2012). Crystallization of lithium disilicate glass using microwave processing. *Journal of the American Ceramic Society*, *95*(2), 579–585. https://doi.org/10.1111/j.1551-2916.2011.04936.x

Mandal, A. K., Agrawal, D., & Sen, R. (2013). Preparation of homogeneous barium borosilicate glass using microwave energy. *Journal of Non-Crystalline Solids*, *371–372*, 41–46. https://doi.org/10.1016/j.jnoncrysol.2013.04.044

Meejitpaisan, P., Kaewjaeng, S., Ruangthaweep, Y., Sangwarantee, N., & Kaewkhao, J. (2021). White light emission of gadolinium calcium phosphate oxide and oxyfluoride glasses doped with Dy^{3+}. *Materials Today: Proceedings, 43*, 2574–2587. https://doi.org/10.1016/j.matpr.2020.04.619

Monisha, M., Mazumder, N., Lakshminarayana, G., Mandal, S., & Kamath, S. D. (2021). Energy transfer and luminescence study of Dy^{3+} doped zinc-aluminoborosilicate glasses for white light emission. *Ceramics International, 47*(1), 598–610. https://doi.org/10.1016/j.ceramint.2020.08.167

Pawar, P. P., Munishwar, S. R., Gautam, S., & Gedam, R. S. (2017). Physical, thermal, structural and optical properties of Dy^{3+} doped lithium alumino-borate glasses for bright W-LED. *Journal of Luminescence, 183*, 79–88. https://doi.org/10.1016/j.jlumin.2016.11.027

Pawar, P. P., Munishwar, S. R., & Gedam, R. S. (2017). Intense white light luminescent Dy^{3+} doped lithium borate glasses for W-LED: A correlation between physical, thermal, structural and optical properties. *Solid State Sciences, 64*, 41–50. https://doi.org/10.1016/j.solidstatesciences.2016.12.009

Poonam, Shivani, Anu, Kumar, A., Sahu, M. K., Rani, P. R., Deopa, N., Punia, R., & Rao, A. S. (2020). Judd-Ofelt parameterization and luminescence characterization of Dy^{3+} doped oxyfluoride lithium zinc borosilicate glasses for lasers and w-LEDs. *Journal of Non-Crystalline Solids, 544*, 120187. https://doi.org/10.1016/j.jnoncrysol.2020.120187

Pugliese, D., Boetti, N. G., Lousteau, J., Ceci-Ginistrelli, E., Bertone, E., Geobaldo, F., & Milanese, D. (2016). Concentration quenching in an Er-doped phosphate glass for compact optical lasers and amplifiers. *Journal of Alloys and Compounds, 657*, 678–683. https://doi.org/10.1016/j.jallcom.2015.10.126

Rajagukguk, J., Sarumaha, C. S., Chanthima, N., Wantana, N., Kothan, S., Wongdamnern, N., & Kaewkhao, J. (2021). Radio and photo luminescence of Dy^{3+} doped lithium fluorophosphate scintillating glass. *Radiation Physics and Chemistry, 185*, 109520. https://doi.org/10.1016/j.radphyschem.2021.109520

Rajagukguk, J., Yuliantini, L., Fitrilawati, Djamal, M., & Kaewkhao, J. (2020). Investigation of Dy^{3+} ion doped borate glasses and their potential for WLED and laser application. *Journal of Engineering and Technological Sciences, 52*(6), 891–906. https://doi.org/10.5614/j.eng.technol.sci.2020.52.6.9

Rao, T. V. R., Reddy, R. R., Nazeer Ahammed, Y., Parandamaiah, M., Sooraj Hussain, N., Buddhudu, S., & Purandar, K. (2000). Luminescence properties of Nd^{3+}: TeO_2–B_2O_3–P_2O_5–Li_2O glass. *Infrared Physics & Technology, 41*(4), 247–258.

Ratep, A., & Kashif, I. (2023). Judd–Ofelt and luminescence properties of dysprosium and terbium doped bismuth-borate glass system. *Optical and Quantum Electronics, 55*(6), 559. https://doi.org/10.1007/s11082-023-04725-9

Sarumaha, C. S., Kaewnuam, E., Lertloypanyachai, P., Srisittipokakun, N., Kim, H. J., Intachai, N., Kothan, S., & Kaewkhao, J. (2025). Novel Ce^{3+}/Dy^{3+} co-doped RHA double-function glasses for UV protection and white light emission capability. *Journal of Alloys and Compounds, 1020*, 179261. https://doi.org/10.1016/j.jallcom.2025.179261

Sevast'yanov, R. I. (1994). Use of electric power in glass melting. *Glass and Ceramics, 51*, 105–108. https://doi.org/10.1007/BF00680071

Shoaib, M., Rajaramakrishna, R., Rooh, G., Chanthima, N., Kim, H. J., Saiyasombat, C., Botta, R., Nuntawong, N., Kothan, S., & Kaewkhao, J. (2020). Structural and luminescence study of Dy^{3+} doped phosphate glasses for solid state lighting applications. *Optical Materials, 109*, 110322. https://doi.org/10.1016/j.optmat.2020.110322

Singkiburin, N., Srisittipokakun, N., Rajaramakrishna, R., Kothan, S., Intachai, N., & Kaewkhao, J. (2023). Investigation of europium oxide (Eu_2O_3) doped in cobalt boro-silicate glasses from waste glass for photonics material application. *Optik, 291*, 171146. https://doi.org/10.1016/j.ijleo.2023.171146

Sreedhar, V. B., Ramachari, D., & Jayasankar, C. K. (2013). Optical properties of zincfluorophosphate glasses doped with Dy^{3+} ions. *Physica B: Condensed Matter, 408*(1), 158–163. https://doi.org/10.1016/j.physb.2012.09.047

Srihari, T., & Jayasankar, C. K. (2017). Fluorescence properties and white light generation from Dy^{3+}-doped niobium phosphate glasses. *Optical Materials, 69*, 87–95. https://doi.org/10.1016/j.optmat.2017.04.001

Sun, Y., Yu, F., Liao, M., Ma, J., Wang, X., He, D., Gao, W., Knight, J., & Hu, L. (2020). Visible emission and energy transfer in Tb^{3+}/Dy^{3+} co-doped phosphate glasses. *Journal of the American Ceramic Society, 103*(12), 6847–6859. https://doi.org/10.1111/jace.17391

Venkata Rao, K., Babu, S., Venkataiah, G., & Ratnakaram, Y. C. (2015). Optical spectroscopy of Dy^{3+} doped borate glasses for luminescence applications. *Journal of Molecular Structure, 1094*, 274–280. https://doi.org/10.1016/j.molstruc.2015.04.015

Venugopal, A. R., Rajaramakrishna, R., Rajashekara, K. M., Rajaguguk, J., Ayachit, N. H., Kothan, S., & Kaewkhao, J. (2021). Dy^{3+} doped B_2O_3 – Li_2O – CaO – CaF_2 glass for efficient white light emitting sources. *Journal of Non-Crystalline Solids, 554*, 120604. https://doi.org/ 10.1016/j.jnoncrysol.2020.120604

Vijayakumar, M., Mahesvaran, K., Patel, D. K., Arunkumar, S., & Marimuthu, K. (2014). Structural and optical properties of Dy^{3+} doped aluminofluoroborophosphate glasses for white light applications. *Optical Materials, 37*, 695–705. https://doi.org/10.1016/j.optmat.2014.08.015

Vijayakumar, M., & Marimuthu, K. (2015). Structural and luminescence properties of Dy^{3+} doped oxyfluoro-borophosphate glasses for lasing materials and white LEDs. *Journal of Alloys and Compounds, 629*, 230–241. https://doi.org/10.1016/j.jallcom.2014.12.214

Vijayakumar, R., Venkataiah, G., & Marimuthu, K. (2015). Structural and luminescence studies on Dy^{3+} doped boro-phosphate glasses for white LED's and laser applications. *Journal of Alloys and Compounds, 652*, 234–243. https://doi.org/10.1016/j.jallcom.2015.08.219

Wantana, N., Chamlek, O., Chanthima, N., Jayasankar, C. K., Kim, H. J., Djamal, M., & Kaewkhao, J. (2016). Spectroscopic properties and Judd-Ofelt analysis of Dy^{3+} in lithium lanthanum borate glass for laser medium application. *Key Engineering Materials, 675–676*, 389–392.

Zaman, F., Khan, I., Khattak, S. A., Kaewkhao, J., Ataullah, Shoaib, M., Shah, A., & Rooh, G. (2019). Investigation of luminescence and lasing properties of Dy^{3+}-doped-borate glasses for white light generation. *Solid State Sciences, 90*, 68–75. https://doi.org/10.1016/j.solidstatesciences.2019.02.006